Journal of Engineering Science and Technology
Vol. 10, No.12 (2015) 1575 - 1588

STUDY ON THE OPTIMIZATION OF IGBT THERMAL MANAGEMENT FOR PTC HEATER

J. W. JEONG, Y. L. LEE*

Dept. of Mechanical Engineering, Kongju National University
Chungnam, South Korea
*Corresponding Author: ylee@kongju.ac.kr

Abstract

It is essential to optimize HVAC (Heating, Ventilation and Air-Conditioning) system for a thermal plant or an electric vehicle since it has a significant effect on the thermal efficiency. PTC (positive temperature coefficient) heaters are often used for a heating system and the power module of the PTC heaters, IGBT (insulated gate bipolar mode transistor), requires thermal management. In this study, in order to maximize the cooling performance for IGBT, a novel method that uses forced convection inside the HVAC duct with heat sinks was developed. In addition, heat sinks were optimized in terms of IGBT junction temperature and heat sink weight by 3-dimensional CFD (Computational Fluid Dynamics) simulation. The results show that the junction temperature of IGBT for 5.6kW PTC heater can be maintained at about 335K.

Keywords: HVAC (heating, ventilation and air-conditioning), PTC (positive temperature coefficient), IGBT (insulated gate bipolar mode transistor), Heat sink

1. Introduction

Environmental problems are among the greatest challenges of our time. In particular, we are now faced with various problems caused by global warming. The average temperature of the earth has long been maintained at 15°C. However, with rapid industrialization, the earth's average temperature has risen 0.5°C over the past 20 years due to the rise of greenhouse gases (GHG), and is expected to further increase by up to 6.4°C by the end of the 21st century [1]. Consequences of this include that the convection currents between the equator and both poles

Abbreviations

BAU	Business As Usual
CFD	Computational Fluid Dynamics
HVAC	Heating, Ventilation and Air Conditioning
IGBT	Insulated Gate Bipolar mode Transistor
IPCC	Intergovernmental Panel on Climate Change
PTC	Positive Temperature Coefficient

will be reduced, leading to more frequent natural disasters such as drought, typhoons, and tsunamis.

It is estimated that global GHG emission in 2030 will increase by 25-90% compared to 2000 level. Also, CO_2-equivalent concentrations are expected to grow to as much as 600-1550 ppm [2]. In response to this environmental challenge, advanced countries have set their respective targets for reduction of their CO_2 emissions based on the IPCC (Intergovernmental Panel on Climate Change) Convention while strengthening related regulations.

South Korea has decided to reduce its GHG emissions by 30% from the BAU (Business As Usual) level by 2020, and launched a target management system for GHG and energy. This has drawn attention to the need for the development of environment-friendly vehicles, in particular, electric vehicles [3].

Electric vehicles do not use fossil fuels, and accordingly do not emit CO_2 [4]. However, when the air-conditioning/heating system of an electric vehicle is operated, its driving distance is reduced by up to 63%. Therefore, the development of a HAVC system for electric vehicles is essential [2]. While the temperature of the coolant used for vehicles with an internal combustion engine is about 100°C, the temperature is only 60°C in the case of electric vehicles [5]. Therefore, the existing heating system cannot be applied. As an alternative, the PTC heater is now drawing attention. Figure 1 shows the PTC heater used in electric vehicles. As shown in Fig. 2 when the temperature reaches a certain point, the resistance of the PTC thermistor increases rapidly, enabling fast heating [6]. In addition, as the current can be controlled depending on ambient temperature, fire due to overheating can be prevented.

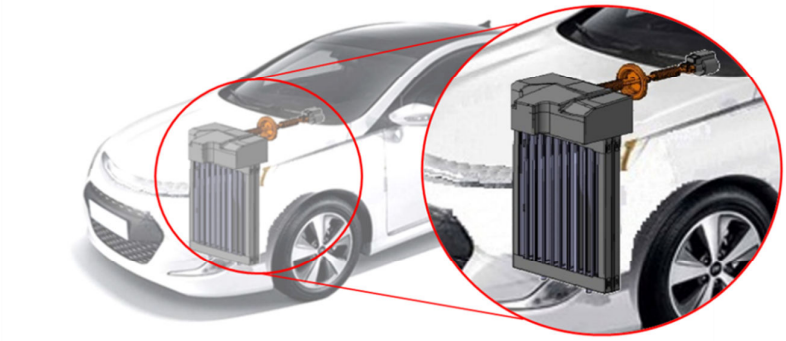

Fig. 1. Schematic of PTC heater in an electric vehicle.

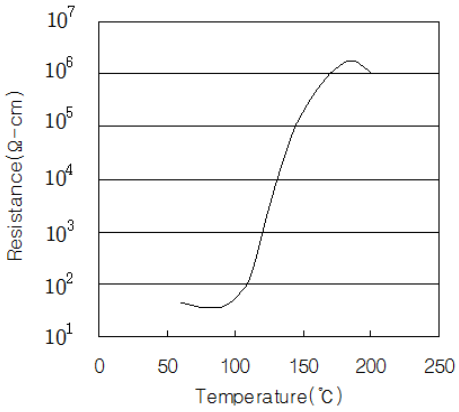

Fig. 2. PTC resistance characteristics with temperature [4].

The PTC heater uses an IGBT as a power module, which changes low voltage to high voltage, causing significant heat [7, 8]. Therefore, for safe operation of the IGBT, thermal design for limiting the junction temperature to a maximum allowable temperature set by the manufacturer [9] is essential. Generally, heat rejection devices such as a heat sink and a heat exchanger are used for thermal design, and the velocity, surface area and weight of the heat sink or the heat exchanger are important factors that determine the heat rejection performance [10 - 12]. No research has been done to cool the IGBT of the PTC heater with a heat sink or a heat exchanger that utilizes HVAC duct flows.

Thus, in this study, for optimization of the IGBT heat rejection performance of the PTC heater, forced convention of a HVAC fan is applied to the IGBT heat sink. Also, efforts have been made to reduce the weight of the IGBT heat sink. To this end, optimization of the junction temperature and weight according to shape changes of the heat sink has been pursued. The target junction temperature of the IGBT has been assumed to be 365K by the manufacturer's datasheet [9].

2. Numerical Methods

For a heat flow analysis of a heat sink, a numerical analysis was performed based on 3-dimensional, steady and turbulent flows. The k-ε realizable model was used for turbulent flows, and the discrete ordinate (DO) model was applied for radiation heat transfer [11, 12]. The material properties used for simulation are listed in Table 1.

Figure 3 shows the boundary conditions used in this study, where the following was assumed: ambient temperature of 313K (engine room temperature); flow rate at the HAVC duct inlet of 359 CMH; and atmospheric pressure for the HAVC duct outlet. The HAVC duct was assumed to be a wall. Each IGBT dissipates heat of 5600W.

Figure 4 shows the analysis model. Model 1 is an IGBT without a heat sink, and Models 2, 3, and 4 are a plain heat sink with thickness of 2 mm, 3 mm, and

4mm respectively. Model 5 is a heat sink with thickness of 4mm and circular dimples with depth of 2mm, and Model 6 is a heat sink with thickness of 4mm and elliptical dimples with depth of 2mm. Model 7 is a heat sink with fins with thickness of 2 mm.

Figure 5 shows the mesh system of Model 4. The type of mesh used was a polyhedral mesh. Figure 6 shows the variation of junction temperature with mesh number. The change rate of the junction temperature becomes less than 1 % when the mesh number changes from 400,000 to 500,000. Thus, the mesh number of 500,000 was chosen for analysis. Fluent V14 was used for the numerical analysis.

Table 1. Material properties used for simulation [7].

Geometry	Material	Thermal Conductivity (W/m-K)	Specific Heat (J/Kg-K)	Density (Kg/m^3)
IGBT	Cu	395	385	8960
Pyrogen	Si	153	703	2340
Heatsink	Al	237	910	2702
HAVC duct	FR-4	0.35	1300	1250

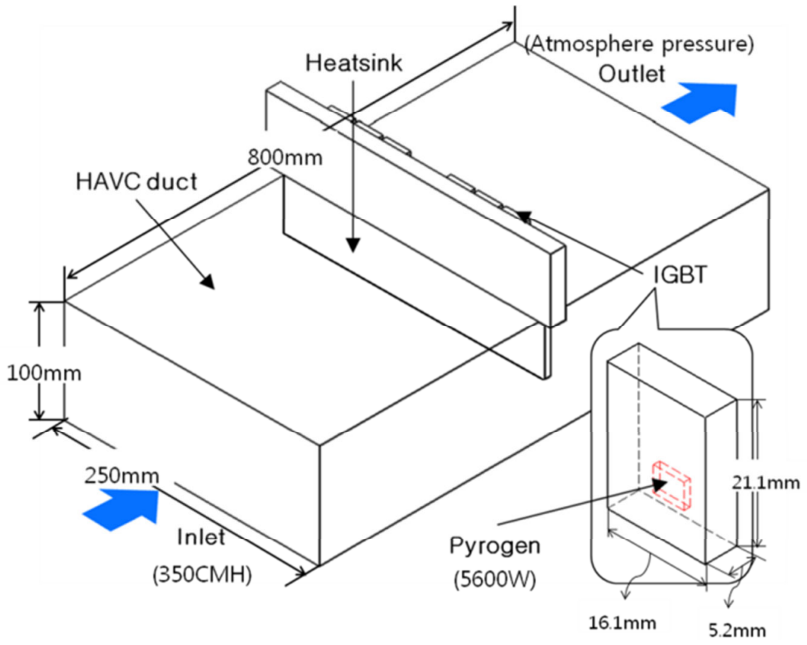

Fig. 3. Schematic and boundary conditions for main model.

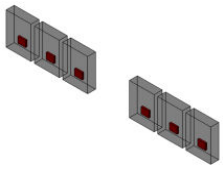

(a) Model 1(IGBT only).

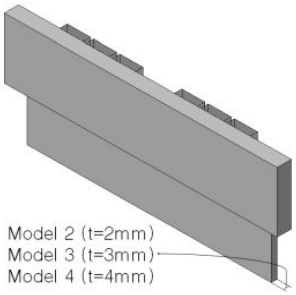

(b) Model 2, 3, 4.

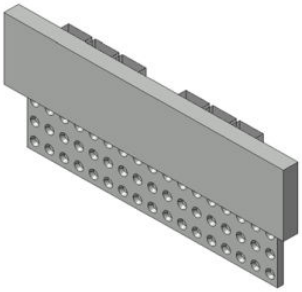

(c) Model 5.

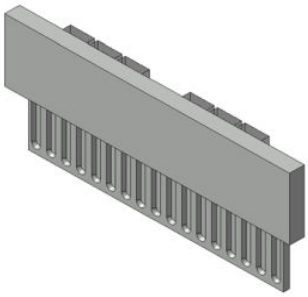

(e) Model 6.

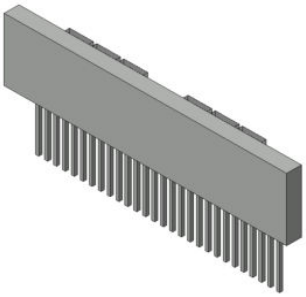

(d) Model 7.

Fig. 4. Schematic illustration of heat sink with model.

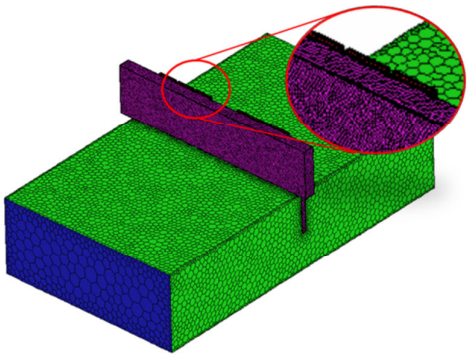

Fig. 5. Mesh system for thermal analysis.

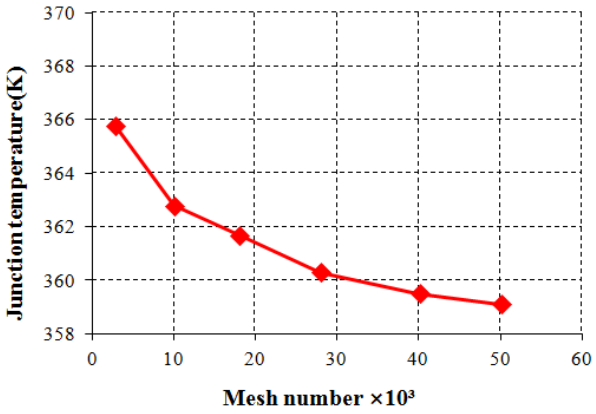

Fig. 6. Variation of junction temperature with mesh number.

3. Results and Discussion

3.1. IGBT Thermal Analysis

The heat rejection performance without a heat sink was studied. In this case, due to the absence of a heat sink, forced convection inside the HAVC duct could not be used for IGBT cooling. Figure 6 shows the velocity vector around the IGBT. The air velocity around the IGBT, which is caused by natural convection, is as high as approximately 0.2 m/s, and this is not sufficient for heat rejection of the IGBT. Figure 7 shows the temperature distribution of the IGBT and the surrounding air. In the case of natural convection, the junction temperature of the IGBT rises up to 490.7K, which is much higher than the maximum junction temperature of 448K set by the IGBT manufacturer. Therefore, additional heat rejection measures are required.

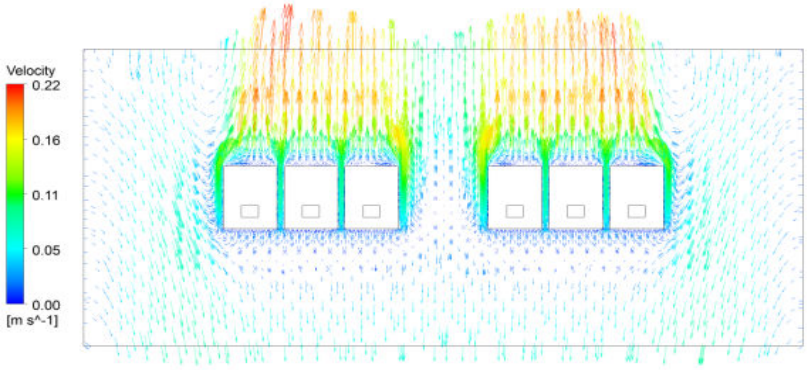

Fig. 6. Velocity vectors for model 1.

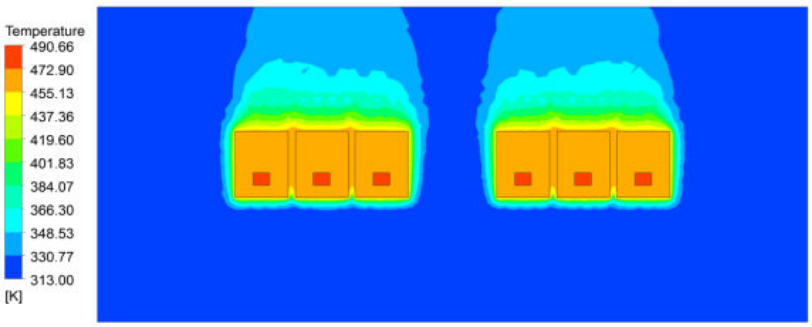

Fig. 7. Temperature contour for model 1.

3.2. Heat Rejection Performance according to Heat Sink Thickness

A heat sink was used to improve the heat rejection performance of the IGBT, and forced convection inside the HAVC duct was used to maximize heat rejection effects. First, the heat rejection performance of the plain-shaped heat sink was reviewed according to thickness. Figure 8 shows the surface temperature distributions by the heat sink model. When the thickness was 2mm, the minimum temperature was 322.9K, and when the thickness was 3mm and 4mm, the minimum temperature was 322.5K and 322.1K respectively. That is, the temperature was reduced by 0.4K for each increase of thickness. This means that increasing thickness does not contribute to improvement of heat rejection performance.

Figure 9 shows the junction temperature according to thickness. When the thickness was 2mm, the junction temperature was 368.1K, and it fell by 1K to 367.1K when the thickness was 3mm and by 2K to 366.4K when the thickness was 4mm. As shown in the figure, the junction temperature decreased as the thickness increased, but the degree of the decrease was small. Figure 10 shows the weight changes according to thickness. When the thickness was 2mm, the weight was 257g, and the weight was increased by 18g to 275g when the thickness was 3mm and by 35g to 292g when the thickness was 4mm. Referring to the figures, as the thickness increased, the degree of the decrease of the junction temperature was relatively smaller compared to the degree of the weight increase, indicating that this approach is not efficient.

3.3. Heat Rejection Performance according to Heat Sink Type

To further optimize the heat rejection performance of the IGBT, different types of heat sinks were applied. Three models were used for the analysis in consideration of junction temperature and weight variation. Figure 11 shows the velocity vector of the forced convection inside the HAVC duct. The maximum speed of the plain heat sink was found to be 25.9m/s, and it was 26m/s and 26.1m/s, respectively, for the heat sink with circular dimples and the heat sink with elliptical dimples. That is, they showed similar maximum speed. However, the maximum speed of the heat sink with fins was reduced by 5.5m/s to 20.4m/s; this indicates that the heat rejection performance was enhanced as the heat sink did not interrupt the flow.

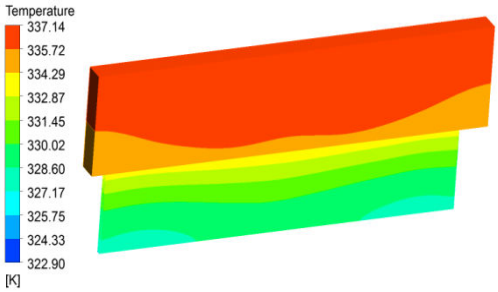

(a) 2mm.

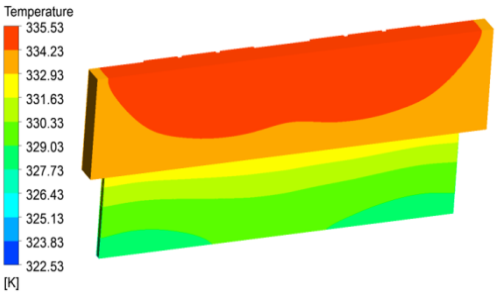

(b) 3mm.

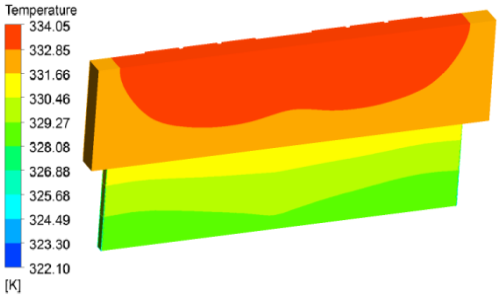

(c) 4mm.

Fig. 8. Temperature contours of models 2, 3, and 4 according to thickness.

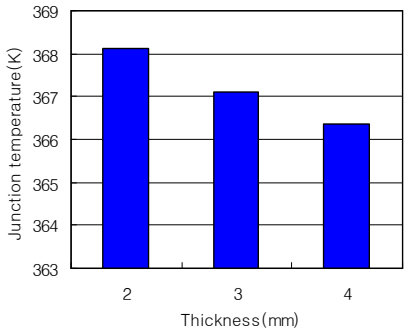

Fig. 9. Variation of junction temperature according to thickness.

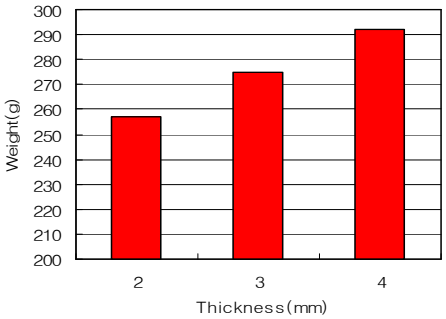

Fig. 10. Variation of heat sink weight according to thickness.

Figure 12 shows the temperature contour according to heat sink type. The minimum temperatures of the heat sink with circular dimples and the heat sink with elliptical dimples were very similar at 322.7K and 322.6K, respectively. Compared to this, the minimum temperature of the heat sink with fins was about 4K lower at 318.9K. This means that the heat sink with fins is more efficient in terms of heat rejection performance. Figure 13 shows the junction temperature according to heat sink type: 364.9K for the heat sink with circular dimples or elliptical dimples, and 365.1K for the heat sink with fins. All three types of heat sink satisfied the target junction temperature.

The heat transfer coefficients are 33, 33.7, 59.8 W/m^2K for circle dimple-type, ellipse dimple-type, fin-type heat sinks, respectively. Thus, the fin-type heat sink has the highest heat transfer coefficient indicating that it is the lightest heats ink among the three. The weight of heat sink is the most important factor in vehicles since it is directly related to fuel efficiency and parts cost [13, 14].

Figure 14 shows the weight according to heat sink type: 287g for the heat sink with circular dimples, 280g for the heat sink with elliptical dimples, and 235g for the heat sink with fins. Therefore, the heat sink with fins is the most efficient as its weight was reduced by 20% relative to the heat sink with circular dimples despite the same junction temperature.

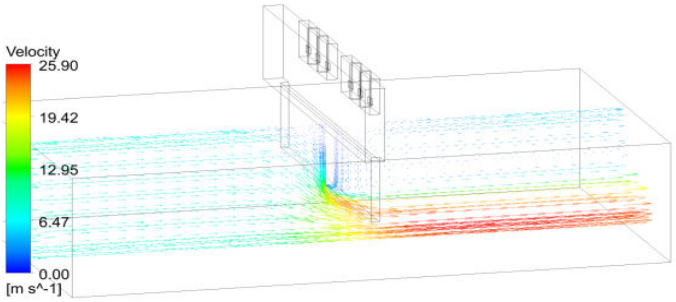

(a) Plain type (t = 4mm).

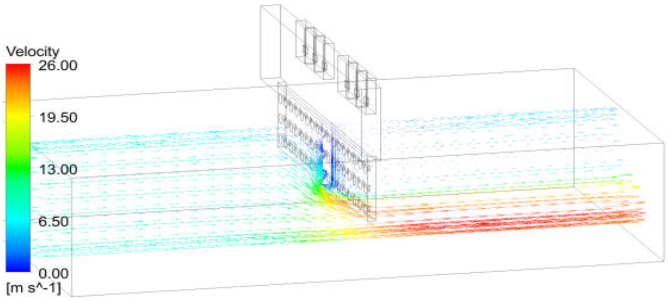

(b) Circular dimple type.

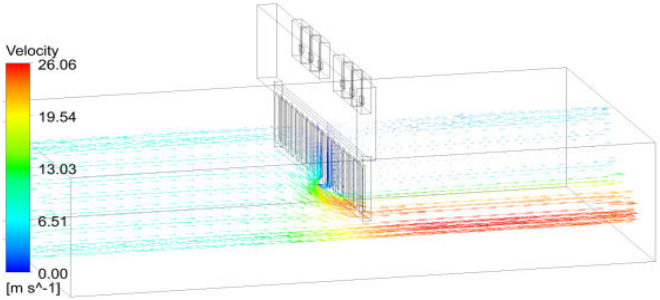

(c) Elliptical dimple type.

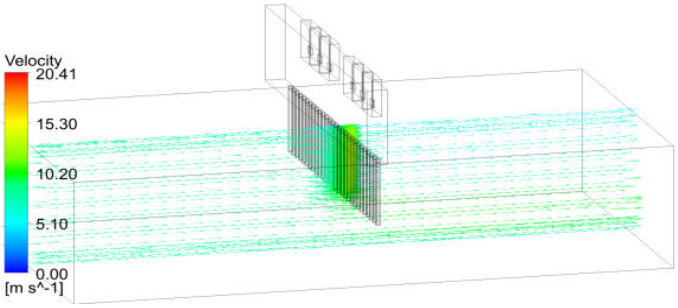

(d) Fin type.

Fig. 11. Velocity vectors according to heat sink type.

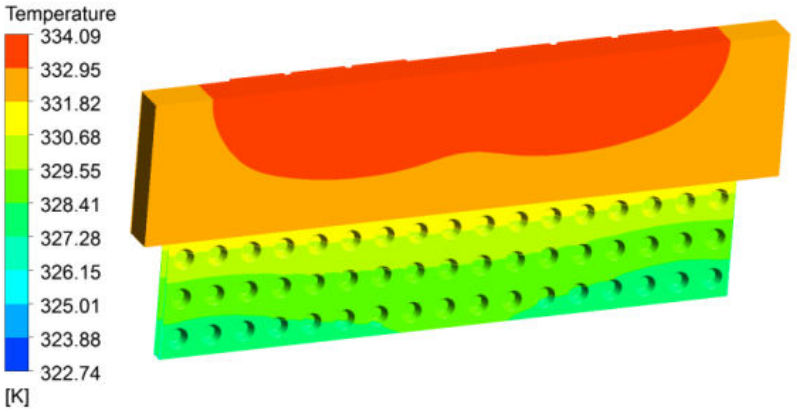

(a) Circular dimple type.

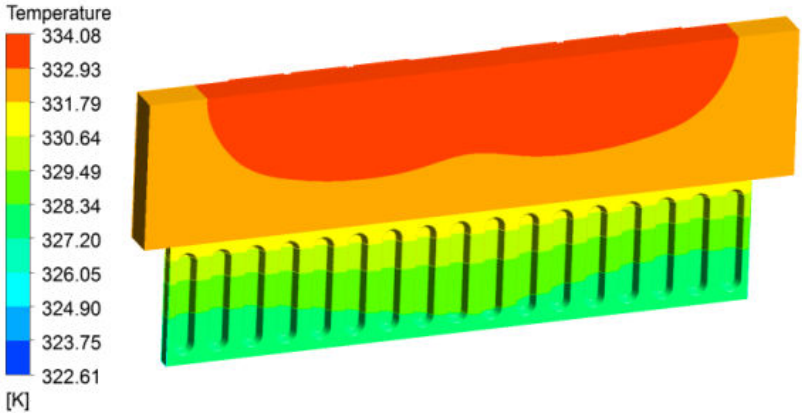

(b) Elliptical dimple type.

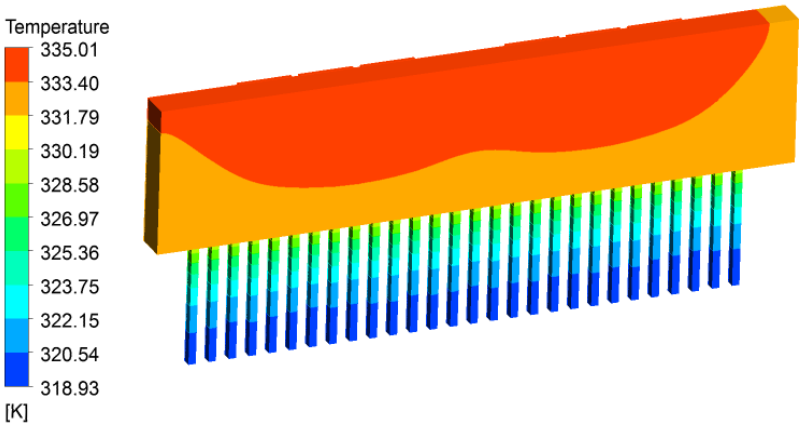

(c) Fin type.

Fig. 12. Temperature contour according to heat sink type.

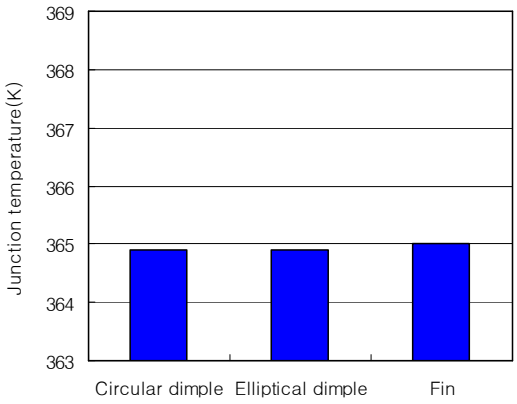

Fig. 13. Variation of junction temperature according to heat sink type.

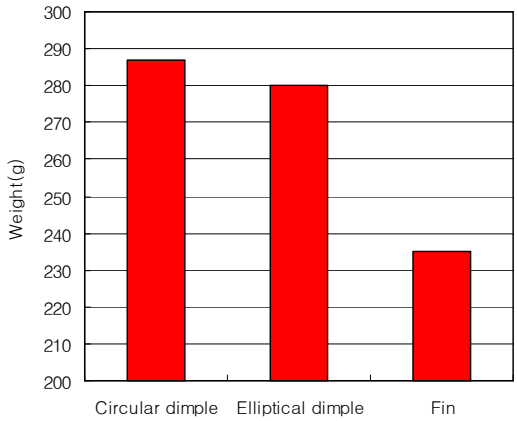

Fig. 14. Variation of weight according to heat sink type.

4. Conclusions

This study aimed to utilize the air current passing through a HAVC duct to maximize the heat rejection performance of an IGBT, which is a power module of the PTC heater of an electric vehicle. To this end, a heat sink was located inside the HAVC duct, and a 3-dimensional numerical analysis was performed by applying diverse heat sink types and shapes. The conclusions of this study are as follows.

- The junction temperature of the IGBT of the PTC heater in an electric vehicle is far higher than the maximum junction temperature set by the manufacturer, requiring additional heat rejection measures.
- Plain heat sinks of different thickness were attached to the IGBT to check the heat rejection performance according to variation of thickness. As the thickness

was increased, the junction temperature fell by 1K only. Therefore, thickness of heat sinks was not efficient to increase heat rejection rate.

- All three types of heat sink (circular dimple, elliptical dimple, and fin) were successful in reducing the junction temperature to the target. However, the heat sink with fins was found to be the most efficient for IGBT cooling in terms of weight and cost.

References

1. Lee, M.I.; and Kang, I.S. (1997). Temperature Variability and Warming Trend in Korea Associated with Global Warming. *Journal of Korean Meteorological Society,* 33(3), 429-443
2. Leung, D.; Caramanna G.; and Maroto-Valer M. (2014). An overview of current status of carbon dioxide capture and storage technologies. *Renewable and Sustainable Energy Reviews,* 39, 426-443
3. Zhou, G.; Ou, X.; and Zhang, X. (2013). Development of electric vehicles use in China: A study from the perspective of life-cycle energy consumption and greenhouse gas emissions. *Energy Policy,* 59, 875-884
4. André, P.; Patríia, B.; Carlos, S.; and Paulo, F. (2014). Energy reduction potential from the shift to electric vehicles : The Flores island case study. *Energy Policy,* 67, 37-47
5. Kim, Y.C.; Sung, N.S.; Jin, K.S.; and Cho, H.T. (2011). Consideration of High Voltage PTC Heater. *KSAE.*, 560-564
6. Seaton, J.; and Leach, C. (2005). Formation and retention of low interfaces in PTC thermistors. *Acta Materialia,* 53, 2751-2758
7. Zhu, J.; Liang, J.; Lua, Y.; and Zhang, C. (2013). A new IGBT control and drive circuit for high-power full-bridge inverter for electrostatic precipitators. *Journal of Electrostatics,* 71, 235-239
8. Ryu, S.H.; Ahn, H.K.; Han, D.K.; and Nokali, M.E. (2007). Thermal analysis of PT IGBT by using ANSYS. *Journal of Power Electrostatics(ICPE)*, 59-61
9. Infineon, from http://www.infineon.com.
10. Li, Y.; Zhang, F.; Sunden, B.; and Xie, G. (2014). Laminar thermal performance of microchannel heat sinks with constructal vertical Y-shaped bifurcation plates. *Applied Thermal Engineering,* 73, 185-195
11. Huang, C.H.; and Chen, Y.H. (2014). An impingement heat sink module design problem in determining simultaneously the optimal non-uniform fin widths and heights. *International Journal of Heat and Mass Transfer,* 73, 627-633
12. Yu, S.H.; Lee, K.S.; and Yook, S.J. (2011). Optimum design of a radial heat sink under natural convection. *International Journal of Heat and Mass Transfer,* 54, 2499-2505
13. Karmare, S.V.; and Tikekarb, A.N. (2010). Analysis of fluid flow and heat transfer in a rib grit roughened surface solar air heater using CFD. *Journal of Solar Energy*, 84(3), 409-417

14. Kumar, S.; and Saini, R.P. (2009). CFD based performance analysis of a solar air heater duct provided with artificial roughness. *Journal of Renewable Energy,* 34(5), 1285-1291
15. O'Keefe, M.; and Bennion, K. (2007). A Comparison of Hybrid Electric Vehicle Power Electronics Cooling Options. *Paper presented at the Vehicle Power and Propulsion Conference,* VPPC 2007, IEEE.
16. Vetrovec, J. (2010). High-Performance Heat Sink for Hybrid Electric Vehicle Inverters. *Paper presented at the ASME 2010 International Design Engineering Technical Conferences and Computers and Information in Engineering Conference.*